DISSERTATIONES CHIMICAE UNIVERSITATIS TARTUENSIS
103

DISSERTATIONES CHIMICAE UNIVERSITATIS TARTUENSIS
103

MARGUS MARANDI

Electroformation of Polypyrrole Films: *In-situ* AFM and STM Study

TARTU UNIVERSITY PRESS

Institute of Chemistry, Faculty of Science and Technology, University of Tartu, Estonia

Dissertation in Inorganic Chemistry

Dissertation is accepted for the commencement of the Degree of Doctor of Philosophy in Chemistry, on March 29 by Council of Institute of Chemistry, University of Tartu

Doctoral advisor:	Prof. Väino Sammelselg, Institute of Chemistry, University of Tartu
	Prof. Jüri Tamm, Institute of Chemistry, University of Tartu
Opponent:	Prof. Mikhael Levi Bar-Ilan University, Israel
Commencement:	May 13, 2011 at 13.00 in Tartu, Ravila 14A, room 1021

Euroopa Liit
Euroopa Sotsiaalfond

Eesti tuleviku heaks

ISSN 1406–0299
ISBN 978–9949–19–630–2 (trükis)
ISBN 978–9949–19–631–9 (PDF)

Tartu Ülikooli Kirjastus
www.tyk.ee
Tellimus nr. 216

TABLE OF CONTENTS

LIST OF ORIGINAL PUBLICATIONS 6

LIST OF ABBREVIATIONS 7

1. INTRODUCTION 8

2. LITERATURE OVERVIEW 10
   2.1. Formation of polypyrrole 10
   2.2. Surface morphology of polypyrrole films 12
      2.2.1. First stages of growth 12
      2.2.2. Surface morphology of thicker PPy films 14
   2.3. Scanning Probe Microscopy methods 15
      2.3.1. Atomic Force Microscopy 15
         2.3.1.1 Contact Mode AFM 15
         2.3.1.2 Dynamic Mode AFM 16
      2.3.2. Scanning Tunnelling Microscopy 17
   2.4. Preparation of well-defined electrode surfaces 18

3. EXPERIMENTAL 19

4. RESULTS AND DISCUSSION 21
   4.1. Adsorbed layer and first stages of polymerisation of Py on Au (111) 21
   4.2. Formation of PPy film on Au (111): A STM and XPS Study 25
   4.3. Dependence of PPy film morphology on different dopant anions 34

5. SUMMARY 39

6. REFERENCES 41

SUMMARY IN ESTONIAN 44

ACKNOWLEDGEMENTS 46

PUBLICATIONS..... 47

LIST OF ORIGINAL PUBLICATIONS

I. M. Marandi, S. Kallip, V. Sammelselg, J. Tamm, AFM study of the adsorption of pyrrole and formation of the polypyrrole film on gold surface; Electrochem. Comm. 12 (2010) 854–858.
Author's contribution: performed or participated in all AFM experiments and performed all electrochemical measurements; participated in writing the paper.

II. M. Marandi, S. Kallip, L. Matisen, J. Tamm, V. Sammelselg, Formation of Nanometric Polypyrrole Films on Au (111): a STM, SEM and XPS Study. Submitted.
Author's contribution: performed or participated in all STM experiments and performed all electrochemical measurements including the synthesis of PPy for XPS mesurements; participated in writing the paper.

III. T. Raudsepp, M. Marandi, T. Tamm, V. Sammelselg, J. Tamm, Study of the factors determining the mobility of ions in the polypyrrole films doped with aromatic sulfonate anions; Electrochim. Acta 53 (2008) 3828–3835.
Author's contribution: performed all AFM experiments; participated in writing the paper.

IV. J. Tamm, T. Raudsepp, M. Marandi, T. Tamm, Electrochemical properties of the polypyrrole films doped with benzenesulfonate; Synth. Met. 157 (2007) 66–73.
Author's contribution: performed all AFM experiments; participated in writing the paper.

V. U. Johanson, M. Marandi, V. Sammelselg, J. Tamm, Electrochemical properties of porphyrin-doped polypyrrole films; J. Electroanal. Chem., 575 (2005) 267–273.
Author's contribution: performed all AFM experiments and performed or participated in all electrochemical measurements; participated in writing the paper.

LIST OF ABBREVIATIONS

Abbreviations	Explanations
AAC-AFM	Acoustic mode AC-AFM
AC-AFM	Dynamic, oscillation probe Atomic Force Microscopy or Microscope
AFM	Atomic Force Microscopy or Microscope
BS^-	Bensenesulphonate anion
CM-AFM	Contact Mode Atomic Force Microscopy or Microscope
CP	Conducting Polymer
CS-AFM	Current-Sensing Atomic Force Microscopy or Microscope
CV	Cyclic Voltammetry
DDS^-	Dodecylsulphate anion
EC-STM	Electrochemical Scanning Tunnelling Microscopy or Microscope
HOPG	Highly Oriented Pyrolytic Graphite
IC-AFM	Intermittent-contact mode Atomic Force Microscopy or Microscope
ITO	Indium tin oxide
MAC-AFM	Magnetic mode AC-AFM
NC-AFM	Non-contact mode Atomic Force Microscopy or Microscope
PAn	Polyaniline
PPy	Polypyrrole
PSS^-	Polystyrenesulphonate anion
PTh	Polytiophene
p-TS^-	*para*-Toluenesulphonate anion
Py	Pyrrole
SEM	Scanning Electron Microscopy or Microscope
SPM	Scanning Probe Microscopy or Microscope
STM	Scanning Tunnelling Microscopy or Microscope
$TPPS_4$	Meso-tetra-(4-sulphonatophenyl)-porphin
XPS	X-ray Photoelectron Spectroscopy

1. INTRODUCTION

Within the last few decades, conducting polymers were intensively investigated as a novel generation of organic materials that have both electrical and optical properties similar to those of metals and inorganic semiconductors, but which also exhibit the attractive properties associated with conventional polymers, such as ease of synthesis and flexibility in processing. The materials have already found applications in a number of advanced technologies, such as chemical sensors, electronic displays, batteries [1,2], etc., and are potent for application in a number of growing new technologies, such as soft polymer actuators or, artificial muscles [3,4]. One popular representative of these conducting polymers is polypyrrole – because of its good stability and ease of preparation by electrochemical polymerisation. In recent time, interest also in nonconductive PPy films has increased, as these can be used as matrixes for biosensors, membranes, molecular sieves, etc. [5,6]. It is important to mark that for the latter applications, very thin films up to few tens of nanometers of thickness are needed today, as the diffusion ability of molecules/ions through the membranes, as well as reaction time of amperometric sensors is inversely proportional to the thickness of the polymer sheet [7].

PPy type polymers can be obtained by the chemical or electrochemical oxidation of the monomer, and it is possible to control some of the polymer properties by varying the experimental conditions. The electronic properties of PPy films can be reversibly electrochemically changed between insulating and conducting states. The electrochemical polymerisation of Py is a complex process, which includes several electrochemical and chemical reactions [8,9].

As is typical of polymers in general, the exact structure of PPy is difficult to determine. It is well known that experimental variables such as dopant, solvent, the applied potential, nature of electrode etc., have a strong influence on the morphology of PPy films. The surface morphology of PPy films synthesised by electrochemical polymerisation is always mainly amorphous. In most cases the bulk PPy film has a “cauliflower” like structure. Differences in roughness and nodule sizes are connected with thickness of the PPy film or the dopant ion.

Scanning probe microscopy is a widely used experimental technique for characterising materials’ surfaces down to the atomic scale. Depending on the measuring method, scanning probe microscopy (SPM) allows to investigate a large variety of materials. Atomic force microscopy (AFM) and scanning tunnelling microscopy (STM) are the two main imaging methods of SPM. During the last years, some essential developments in AFM measurements have been carried out. The less disturbing direct driving magnetic dynamic mode (MAC Mode) appears together with dedicated cantilevers coated with ferro-magnetic thin film [10,11], and this method seems to be the best for AFM imaging in liquids, for examination of soft samples like surfactant layers [12], and is also applicable for *in-situ* examination of the adsorption layers of Py.

Despite a large amount of research published using SPM, considering the initial growth mechanism of CP [13–16], the surface morphology as a function

of experimental conditions of electrosynthesis [17,18], the properties of the PPy film [19,20], and the effect of the doping state in the polymer morphology [21], there has been no complete agreement about the mechanisms of growth of PPy at the moment of beginning this study.

The main aim of the present investigation was to study the first stages of PPy film growth on Au electrode for the better understanding of the film formation mechanisms and properties of ultrathin films, thus, it was important to examine the adsorption process of Py on atomically flat Au (111) surface from, commonly used, moderate concentration (0.1 M), and more diluted (0.1 and 1 mM) aqueous solutions of Py, and to study the first stages of growth of the electropolymerised PPy structures from the adsorbed Py layer. From the other side the surface structure and other properties of thicker films may be influenced by not only on the film formation during the first stages of its growth but also on the properties of different dopant anions used in the film deposition process: thus, the influence of the dopants to the of thicker film was in the interest as well in this study.

2. LITERATURE OVERVIEW

2.1. Formation of polypyrrole

PPy can be prepared using chemical or electrochemical polymerisation [1,22]. Chemically, Py can be oxidatively polymerised in solution using a wide range of oxidants like $FeCl_3$, Br_2, H_2O_2 and many others. Chemical polymerisation usually leads to powders called "polypyrrole black". Films can be obtained by allowing the polymerisation to take place at a solid or liquid surface. These films are of poor quality, in some cases they are not even conducting [1,23].

The electrochemical polymerisation is generally preferred because it provides a better control of film thickness and morphology and a cleaner polymer when compared to the chemical oxidation. Films of PPy are deposited onto a supporting electrode surface by anodic oxidation of Py in the presence of an electrolyte solution. The choice of the solvent and electrolyte is very important in the electrochemical polymerisation of PPy, because both of them should be stable at the oxidation potential of Py and provide a conductive medium. The anode can be made of a large variety of materials including gold, platinum, glassy carbon, HOPG, and ITO coated glass, etc. Electrochemical polymerisation can be carried out using different electrochemical methods like potentiostatic, galvanostatic or potentiodynamic methods.

The electrochemical polymerisation reaction can be described with following equation:

$$\mathbf{4n\ H\text{-}M\text{-}H + nA^- - (9n\text{-}2)e^- \rightarrow H\text{-}(M)_{4n}{}^{n+}\text{-}H/nA^- + (8n - 2)H^+}$$

where H-M-H represents monomer, A^- represents anion from electrolyte and H-$(M)_{4n}{}^{n+}$-H represents polycation formed from monomers. According to this equation, a large amount of hydrogen ions are produced during polymerisation reaction, which is confirmed by the observed pH drop of the solution during polymerisation [8].

The electropolymerisation mechanism of Py is not very clear. Up to date, a number of mechanisms of these reactions have been proposed [8]. The mechanism described by Diaz et al. is the mechanism encountered most often in the literature [24,25]. The scheme of this polymerisation mechanism is shown in Scheme 1. According to the scheme, the polymerisation begins by the oxidation of the monomer at the surface of the electrode to form the radical cation. The coupling between two radicals results in the formation of the dihydromer dication. Than the loss of two protons forms the aromatic dimer. There is two preferred ways for describing the further extension of polymer chain. One theory says that the elongation of polymer chain is based on the successive coupling of monomeric cations with the chain as shown in Scheme 1 [24,25]. According to the second theory, the propagation of PPy chain takes place via

successive dimerisation steps leading from a dimer to a tetramer and then to an octameric coupling product (Scheme 2)[9].

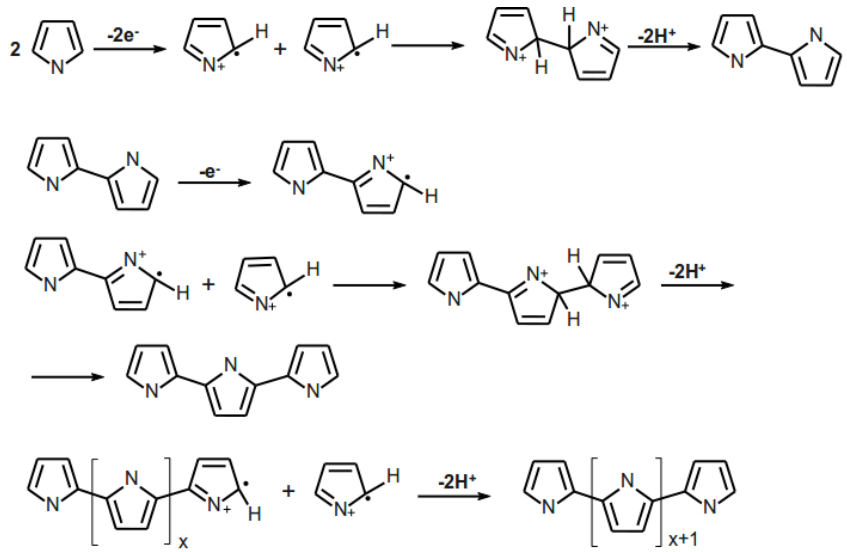

Scheme 1. Classical formation scheme during oxidation of Py.

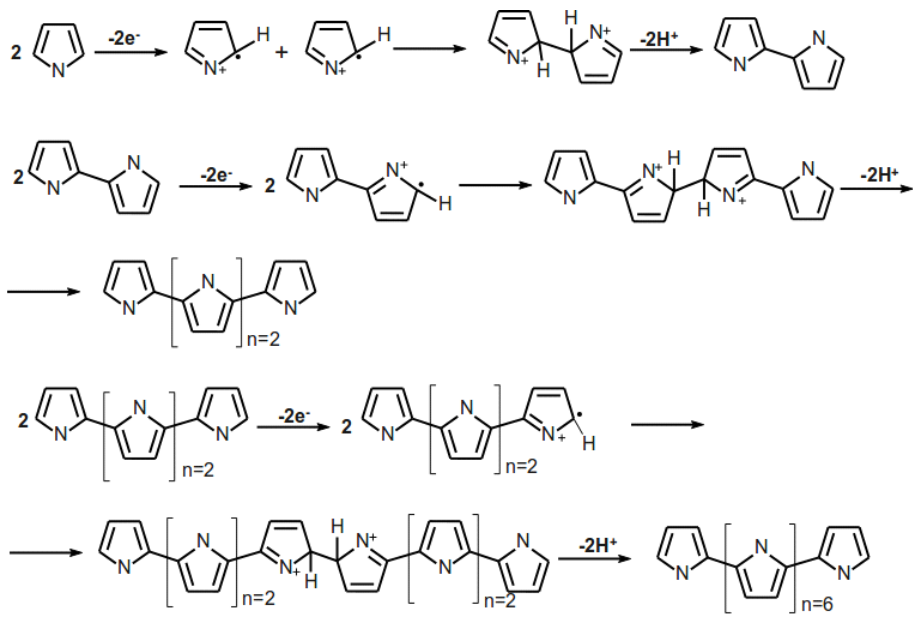

Scheme 2. PPy formation scheme via oligomerisation.

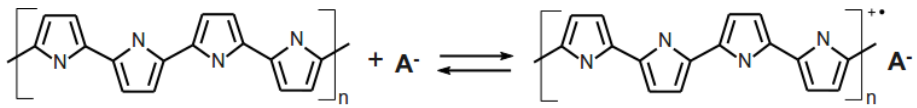

Scheme 3. Structure of doped polymer.

The electropolymerisation does not give the neutral non-conducting PPy but its oxidised conducting form. The final polymer chain carries a positive charge for every 5 to 3 Py units, which is neutralised by an anion. The structure of doped polymer is presented in Scheme 3, where A^- is the electrolyte anion [8].

As mentioned, the electropolymerisation mechanism is a controversial subject. Difficulties in the determination of the different stages of the reaction are related with the rapidity of the polymerisation. The insolubility of the PPy coupled with its non-crystalline nature makes structure characterisation and analysis of physical properties extremely difficult. As a result, there is no unanimous agreement concerning this mechanism.

2.2. Surface morphology of polypyrrole films

Experimental variables such as dopant, solvent, the applied potential, nature of electrode etc., are known to have a strong influence on the morphology of PPy film. The relationships between these variables and the morphology have been studied because the latter greatly affects the mechanical and electrical properties of the film.

The exact structure of PPy is difficult to determine, as it is typical for polymers in general. The morphology of PPy films synthesised by electrochemical polymerisation changes with the dopant ion and the electrode substrate but the surface is always mainly amorphous [26–28]. Very many experiments for the investigation of the morphology of PPy films/sheets have been done using SEM [29–32]. This measuring method requires thicker films for the investigations – mostly 1 μm or thicker films are usually studied. The very early stages of PPy growth cannot be studied by standard SEM. In most cases, the thicker films have a “cauliflower” like structure. Differences in roughness and nodule sizes are connected with the thickness of PPy film or dopant ion. If the thickness of PPy film increases, the roughness of film surface increases as well.

Since the inventing, the SPM has proven useful for the determination of surface properties of PPy.

2.2.1. First stages of growth

The morphology changes of PPy films on different polycrystalline electrodes and different dopant anions during first stages of PPy growth have been

investigated using *in-situ* SPM in a few early studies [33–35]. The formation of a thin polymer layer over the whole Pt electrode area during the first stage of PPy synthesis was observed [33]. Quite similar observations have been done on the basis of *ex-situ* STM experiments on polycrystalline Pt electrodes [34]. This corroborates the opinion that the initial growth of PPy film is essentially two dimensional, the PPy chain structure grows preferentially on the electrode surface until it coats the whole surface. The growth of nodules occurred after the formation of a polymer thin layer. Different morphology of the PPy films developed over different electrodes was shown [34]. Unordered structure of PPy film was observed over Pt electrodes, more ordered oval structures were observed over glassy carbon electrode during the initial stages of synthesis in the presence of ClO_4^- or *p*-TS^- anions. Highly oriented growth of nuclei of PPy was seen over a gold electrode in the presence of ClO_4^-. A very uniform thin PPy film has also been detected in the first stage of polymerisation in another *in-situ* AFM study of the polymerisation of Py on Au (111) film vapor deposited on glass substrate [35]. The STM *ex-situ* experiments of other conducting polymers have shown that the initial deposition step of these polymers on gold is the formation of a very regular, very stable and adherent thin film [36]. It has been noticed that the growth of PPy over glassy carbon and gold electrodes is more homogeneous than over platinum electrodes. Also, the synthesis of PPy over glassy carbon and gold electrodes has demonstrated that the scratch lines over the electrode did not offer evident advantage for the nucleation of the polymer. These experiments have suggested that there are two stages during the growth of PPy films. First, there is the deposition of a primary PPy layer, which occurs, either via polymerisation of adsorbed species on the electrode, or by deposition of oligomers on the latter. The second stage concerns the growth of this layer.

Different results have been achieved with *ex-situ* STM measurements in the first stages of PPy polymerisation on HOPG electrode [13,37–39]. There the formation of ultra thin PPy layer on the electrode surface has not been detected. Variety of structural forms of electropolymerised PPy with small counterions has been showed on HOPG: isolated helical polymer chains with pitches of 0.5–0.9 nm and diameters of 1.5–1.8 nm, small nodules with diameters up to 100 nm consisting of crystalline ordered arrays of supercoils were found. These nodules of PPy typically have been found on or near the surface steps of the graphite. Also, the formation of polymer strands, which are in some cases isolated and in others attached to the nodules have been observed. Similar coil and nodular structures have been observed in thin films of PTh on HOPG [13] and PAn on Pt electrode [40]. By studying PPy electropolymerised with large polymeric anion like PSS^-, it has been found that thin films and nodules formed in the early growth stage posses crystalline structure [38].

The AFM *ex-situ* experiments on Pt single-crystal electrodes with basal orientations have shown that the formation of PPy is a structure-sensitive process [41]. It was clearly shown that the morphology of the PPy deposits on the three basal planes of Pt electrodes is very different. Highly heterogeneous

polymer film was formed on Pt (100) with zones completely covered by thick polymer film and zones with low coverage where a very thin film was present. On Pt (110) a very homogeneous film formation was observed, and on the Pt (111) new types of wide terraces of PPy with a shape usually described as fingers were formed. It was found that the Pt (110) and Pt (111) surfaces are more suitable for obtaining PPy films with higher conductivity and charge-storage capacity than Pt (100) surface.

Electrical properties of PPy films studied under various experimental conditions by Park et al. [42–44] showed that at the very early stage of the film growth (~10 nm) in aqueous solutions, the surface of the electrode is almost fully covered with a nonconducting thin layer. It was presumed that this layer consists probably of undoped or poorly doped short-chained PPy and/or Py oligomers at this stage. When the thickness of PPy films was increased, the conductivity of these films increases too.

2.2.2. Surface morphology of thicker PPy films

The influence of dopant nature and film thickness on the roughness of PPy films has been studied *ex-situ* by AFM [45,46] and STM [14,38,39]. During the STM measurements at intermediate PPy film thicknesses (20–90 nm) on HOPG, a fibrillar structure was observed which transformed with the increasing film thickness into the nodular amorphous polymer structure. The sizes of the nodules increased with film thickness and were found to be similar to the structures observed by other surface characterisation methods. AFM experiments showed that the surface morphology of PPy films doped with various anions (Cl^-, ClO_4^-, SO_4^{2-}, DDS^-) is less affected by the nature of the dopant at film thicknesses below 1μm where the first polymer particles on the surface are globular and oriented along scratch lines on the substrate electrode. Remarkable differences become evident for thicker films: the behaviour of globules doped with sulphate or DDS^- anions follows that obtained for relationship of thinner films, but in the case of chloride-doped and perchlorate-doped films a sharp increase in diameter and height of globules have been obtained.

Electrical and morphological properties of PPy films have been studied using a current sensing AFM (CS-AFM) on a nanometer scale [42–44]. These experiments have clearly demonstrated that the PPy films prepared in aqueous electrolyte solutions were in general inhomogeneous in their electrical properties showing much poorer conductivities than those prepared in acetonitrile. When the thickness of PPy films was increased, the conductivity of these films increases as well. Also, the role of electrolyte in determining the morphological and electrical properties of the PPy films was investigated. The thickness of the polymer prepared in various electrolyte solutions was depending on them in order of SDS^->PSS^->*p*-TS^->ClO_4^- for an identical amount of anodic charges used for the preparation. The average conductance values gave the order of *p*-TS^->SDS^->PSS^->ClO_4^-. It has been concluded that the morphological and

electrical characteristics of PPy films can be as diverse as the experimental conditions [43].

2.3. Scanning Probe Microscopy methods

Scanning probe microscopy is a widely used experimental technique for characterising materials' surfaces down to the atomic scale. Depending on measuring method, SPM allows investigate large variety of materials. It is possible to carry out SPM experiments in very different environments – in ultra high vacuum, controlled gas environment, ambient conditions and liquids [47].

In SPM techniques, the sharp probe is either scanned across a sample or the surface is scanned beneath the probe. Interactions between the tip and the sample are detected and mapped. Different techniques sense different interactions, which can be used to describe surface topography, adhesion, elasticity, conductivity, etc.

Atomic Force Microscopy and Scanning Tunnelling Microscopy are the two main imaging methods of SPM.

2.3.1. Atomic Force Microscopy

AFM can resolve features as small as an atomic lattice, for either conductive or non-conductive samples. The technique makes it possible to image the samples *in-situ*, in fluid, under controlled environments. AFM imaging relies on small AFM probe that is raster scanned over a surface to generate an AFM image. AFM probes have two major components; a flexible cantilever, which is attached to the probe chip, and a sharp probe tip near the end of the cantilever. AFM probes can be manufactured from a variety of materials, but are mostly made of silicon and/or silicon nitride. The tip diameter can vary, depending on its specific application, but it is generally extremely sharp, usually on the order of a few nanometers to tens of nanometers in radius at the tip apex. Various novel techniques have been developed for creating even sharper tips; for example, carbon nanotubes have been added to the end of the probes. The potential of AFM extends to applications in life science, material science, electrochemistry, polymer science, nanotechnology, biotechnology, etc. [48–50].

Contact mode (CM) and dynamic (AC) mode are two major AFM imaging modes.

2.3.1.1. Contact Mode AFM

In contact mode, the AFM probe tip is in continuous contact with the sample. Typically, the forces applied to samples in CM are in the range from tens to hundreds of nano-Newtons (nN). Additionally, most surfaces in air are covered by a layer of adsorbed water and other contaminants, whose surface tension

pulls the tip and probe downwards by capillary, adhesion, and etc. forces. Electrostatic charges on the tip and sample can also give rise to additional long-range forces and complicate the imaging. When scanning in fluids, for example under water or solution of different salts, the capillary forces are eliminated, and the electrostatic forces are largely screened. Consequently, experiments under liquids could be easier to carry out and less damaging for the sample than at ambient conditions as relatively large vertical and lateral forces, which are applied to the sample during CM imaging, can often damage soft or weakly attached samples.

2.3.1.2. Dynamic Mode AFM

In contrast to CM, in AC or dynamic mode (AC-AFM) the AFM probe is oscillated at a high frequency above the sample. One advantage of this mode is that the probe does not contact at all or contacts very slightly and/or shortly with the sample surface.

There are two main AC imaging techniques of AC-AFM, the acoustic (AAC) and magnetic (MAC) AC techniques. In AAC mode, a piezoelectric transducer is used to oscillate the AFM probe near its resonant frequency. In liquids, an amplitude vs frequency resonance sweep for an AFM probe that is driven to resonance in AAC mode is described as a "forest of peaks" (Fig. 1. a) [51]. This is because the transducer tends to vibrate not only the AFM probe, but also the surrounding environment and items that happen to be in close proximity to the transducer. This effect can make it difficult to find the true resonant frequency of the probe, and also to optimise other imaging parameters. With MAC mode, a special magnetically coated cantilever is driven by an oscillating magnetic field. There is low or no "forest of peaks" for amplitude vs frequency sweep using MAC mode in liquids (Fig. 1. b)[51,52]. The resonant frequency is cleanly resolved as a distinct single peak. The result is more effective, accurate and simpler probe tuning, thus, in MAC Mode compared to other AFM imaging modes, lower imaging forces and much less damage to soft samples occurs. As a result, the MAC mode allows to study samples on the molecular level and image delicate samples which often cannot be resolved with any other AFM imaging technique [11,12,53–55].

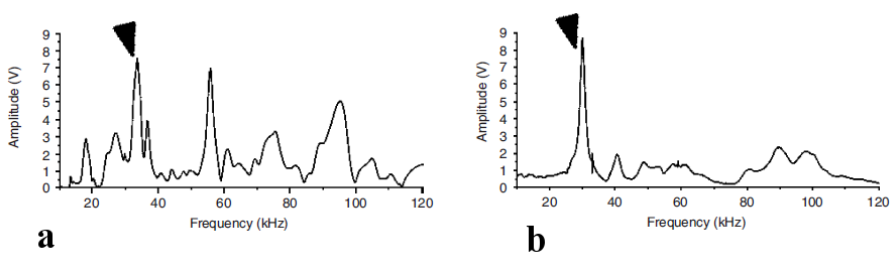

Fig. 1. AAC mode (a) and MAC mode (b) amplitude vs frequency sweep in liquid. [51]

2.3.2. Scanning Tunnelling Microscopy

STM is the earliest, widely-adopted SPM technique. The STM works by scanning a very sharp metal wire tip over a surface. By bringing the tip very close to the surface, and by applying an electrical voltage to the tip or sample, the surface can be imaged at an extremely small scale – down to resolving individual atoms and point defects. The STM is based on the quantum chemical effect of electron tunnelling. The remarkable vertical resolution, up to the picometer range, of the device arises from the exponential dependence on the electron tunnelling current on the tip-substrate separation. For electron tunnelling to occur, both the sample and tip must be conductive or semi-conductive. STM cannot be used on insulating materials. This is one of the significant limitations of STM, which has led to the development of other SPM methods, first of all – the AFM method.

The working principle of *in-situ* STM is that of conventional STM, with the difference that *in-situ* STM equipment is designed to run so that the sample and the tip are placed in a liquid media: the STM tip is dipped into an electrolyte filled electrochemical cell during the image recording. Well-defined *in-situ* experiments require the use of a bipotentiostat to independently control the electrochemical potential of the tip and surface relative to some reference electrode. In an electrochemical environment, the STM tip serves both as a tunnelling probe and as a microelectrode at the same time. Thereby, special attention must be given to the possible faradic reactions at the tip. These reactions may include redox events as well as deposition and dissolution processes. Under constant current imaging conditions, the set point current is maintained by a combination of electron tunnelling and the faradic process occurring at the tip. In order to reduce the faradic contribution at the tip, the sidewall of the tip must be electrically isolated. This is provided by a special tip coating, which leaves only the foremost part of the tip in contact with the liquid [56]. Soft glass, organic polymers, and Apiezon wax have been used for tip coating [57].

The described-above AFM and STM methods are applicable for the examination of the surface morphology of PPy films with some restrictions. As PPy films are relatively soft, contact mode AFM is not the best method for the characterisation of the thin films in *ex-* or *in-situ* studies. There are relatively large vertical and lateral forces applied to the sample during CM-AFM imaging, which can damage the film surface and even partly or completely sweep off the PPy film. Therefore, intermittent- or non-contact AFM methods are preferred for AFM studies of PPy films and specially adsorbed layer of Py. Because of effective, accurate and simpler probe tuning in liquids, the MAC mode is at the moment the favourable method for *in-situ* AFM measurements. Generally, STM allows achieving higher resolution, up to molecular level, for the imaging/measurements of thin PPy films or the adsorbed layer of Py. But there are also some serious problems. The adsorbed layer might be completely swept off by the scanning tip due to too high current densities and/or small distance between tip

and surface, if the adsorbed layer is not enough strongly adhered to the surface of electrode. Also, poor or absence of conductivity of the first stages of film growth may cause problems in STM measurements.

In summary, the best way to perform *in-situ* studies of PPy films or adsorbed layer of Py is to use MAC-AFM or STM. For *ex-situ* experiments NC-AFM is the best choice in case of adsorbed layer or ultrathin films, but for the thicker films also IC-AFM is applicable.

2.4. Preparation of well-defined electrode surfaces

As a rule for the study of polymer film growth on an electrode using STM methods, both electrode-electrolyte interfaces and the surface of the polymer deposited must be well-defined and prepared reproducibly, and methods to investigate these must be established accurately. It is difficult to prepare in very reproducible way as well as to carry out experiments on the atomic scale using polycrystalline electrodes. Thus, well-defined single crystalline surfaces must be exposed in order to understand surface structure on the atomic scale. It is difficult to carry out experiments on the atomic scale using polycrystalline electrodes. At the moment, several methods are achieved to produce extremely well-defined, atomically flat surfaces of various electrodes made of noble metals, some base metals, and semiconductors. One of the widely used methods of preparing a single crystal Pt electrodes is melting of a Pt wire in the flame, which was established by Clavilier et al.[58]. Later, this technique was extended for Au [59], Ir [60], Rh and Pd [61].

Gold films, which were thermally vapor-deposited in vacuum on heated cleaved mica surfaces, are the other way to produce reproducibly well-defined Au (111) single crystal electrodes [62–65]. These kinds of electrodes are frequently used as substrates for the study of biomolecular adsorbates [66], nanoparticle systems [67–69], and SAMs [70–72]. Popularity of these substrates based on simplicity of producing and preparation before experiment. For getting contaminant free atomically flat surface of these substrates only a flame annealing is needed [56,70,71]. The technology of production of reproducible high-quality Au (111) films on mica substrates was introduced in this work as well.

3. EXPERIMENTAL

Pyrrole (Fluka), used for the adsorption of Py layer and synthesis of PPy films, was purified by distillation over calcium hydride under vacuum and stored in the dark under Ar atmosphere at low temperature. All the salts used as dopants ($LiClO_4$, NaCl, NaBS, Na*p*-TS and NaNDS) were analytical reagent grade (mostly products from Fluka). *Meso*-tetra-(4-sulfonatophenyl)-porphine dihydrocloride purchased from Porphyrine Products, Inc. was neutralized with 0.05 M NaOH before use. High purity MilliQ+ water was used for the preparation of solutions.

Monocrystalline Au (111) films were deposited on mica substrates at elevated temperature using electron beam evaporator VS-17 (Vacuumservice OY). The mica substrates had been cleaved just before the preparation. Prior each experiment, the Au (111) electrode was shortly annealed in H_2 flame.

Adsorption of Py was carried out in a one-compartment electrochemical cell from aqueous solutions containing 0.1 M of Py and 0.1 M of $LiClO_4$. Samples were exposed to the Py solution for 3 minutes at open circuit potential. After that the samples were rinsed thoroughly with MilliQ+ water and submerged in 0.1 M $LiClO_4$ solution for *in-situ* AFM measurements. All solutions and MilliQ+ water used in this work were previously saturated with Ar (99.999%, AGA).

Potentiodynamic method was used for the polymerisation of the adsorbed Py layer. Galvanostatically synthesized PPy films for STM and XPS measurements were deposited at constant current density: $j = 0.12\ mA \cdot cm^{-2}$. For XPS measurements, the potentiostatically synthesized film was deposited at constant potential 0.75 V. Electrochemical experiments were carried out using potentiostat/ galvanostat Model 263A (PAR). Mica substrates or Au wire as working electrode, platinum wire as counter electrode and Ag/AgCl reference electrode were used. The estimation of the polymer film thickness was done considering that depending on different dopant anions about 0.2–0.4 $C \cdot cm^{-2}$ is consumed for deposition of 1 μm thick film. [73,74]

The surface morphology of working electrodes was studied by a SPM measurement system 5500 (Agilent Technologies) and Autoprobe CPII (Veeco). *In-situ* AFM experiments were performed in MAC Mode using MACLevers™ type I cantilevers (Agilent Technologies). For *ex-situ* AFM measurements were used Ultralever™ (PSI), NSG11S series (NT-MDT) and SSS-NCHR (Nanosensors™) type cantilevers. All AFM images were recorded in non-contact or intermittent contact mode. The *in-situ* AFM experiments were carried out in 0.1 M $LiClO_4$ supporting electrolyte in a modified hermetic cell. All images were registered at open circuit potential. For *ex-situ* AFM experiments, the samples were rinsed thoroughly with MilliQ+ water and air-dried. STM measurements were carried out with a SPM measurement system 5500 (Agilent Technologies) equipped with electrochemical STM (EC-STM) option. The *in-situ* STM experiments were carried out in 0.1 M Na_2SO_4 supporting electrolyte in a modified hermetic electrochemical cell using insulated Pt/Ir STM tips from

Agilent Technologies, declared having leakage current $i_l < 70$ pA. The *ex-situ* STM experiments were carried out in ambient conditions using etched or cut from Pt/Ir20 wire (Ø 0.25 mm; NanoScience Instruments) tips. All STM images were recorded in constant current mode with tunnelling currents ranging from 1.3 to 19 nA. The GwyddionTM ver. 2.19 [75] free software and WSxM software [76] were employed for image processing. All AFM and STM images were processed by 1st order flattening for background slope removing, and if necessary, the contrast and brightness were adjusted.

XPS measurements were carried out with a UHV surface analysis complex having SCIENTA SES-100 spectrometer with detection angle of 90°. For excitation, an unmonochromated Mg K_α X-ray source (incident energy = 1253.6 eV; power 300 W) was used. The pressure in the analysis chamber was $\sim 5 \cdot 10^{-8}$ Pa. While collecting the survey spectrum, the following spectrometer parameters were used: binding energy range from 600 to 0 eV, pass energy E_p = 200 eV, energy step size ΔE = 0.5 eV. High-resolution photoelectron peaks of interest were scanned in the appropriate energy ranges with energy step of ΔE = 0.1 eV using the same pass energy value. The number of scans over the spectrum energy range used was chosen basing on getting reasonably good statistics of the spectra, and ranged from 2 to 4 for survey spectra and 10 to 40 for high resolution spectra. For the elements, atomic ratio evaluation, experimental line heights were determined and elements' sensitivity factors [77,78] were taken into account.

4. RESULTS AND DISCUSSION

4.1. Adsorbed layer and first stages of polymerisation of Py on Au (111)

AFM and STM images of a typical Au (111) electrode are presented in Fig. 2. It can be seen that the electrode surface is formed by atomically flat (111) terraces limited by monoatomic steps (see the height profile in Fig. 2), and that the terraces are considered to be large enough for detailed studies of Py adsorption and polymerisation. Note that the bare electrode has sharp and typical for the (111) orientation triangular step edges.

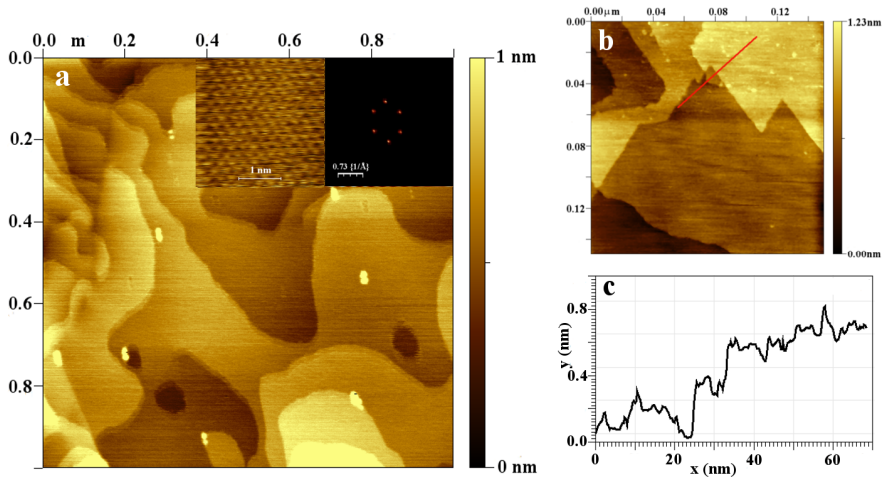

Fig. 2. Typical non-contact AFM (a) and STM (b) images and cross-section profile (c) of Au (111) electrode. Insert in (a): an atomic resolution STM image of a similarly pretreated Au (111) electrode, the left part – raw image, 3 × 3 nm^2, and the right part – FFT pattern of the same image. The RMS surface roughness value measured in image *a* was 0.17 nm. All images were taken in air condition.

Pyrrole (Py) adsorption and following electropolymerisation processes onto partially atomically flat Au (111) surfaces from aqueous solution of 0.1 M Py plus 0.1 M $LiClO_4$ have been investigated by non-contact atomic force microscopy. Adsorption of Py was carried out in a one-compartment electrochemical cell. Samples were exposed to the Py solution for 3 minutes at open circuit potential. After that the samples were rinsed thoroughly with MilliQ+ water and submerged in 0.1 M $LiClO_4$ solution for *in-situ* AFM measurements. All solutions and MilliQ+ water used in these experiments were previously saturated with Ar.

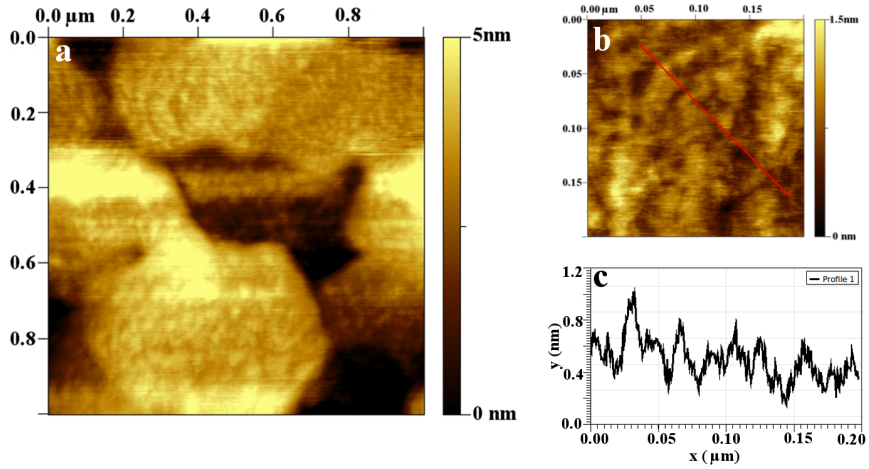

Fig. 3. *In-situ* non-contact AFM images (a,b) and cross-section profile (c) of adsorbed Py layer on Au(111) electrode measured in solution of 0.1 M Py + 0.1 M $LiClO_4$.

Fig. 3 shows *in-situ* AFM image of the Au (111) electrode surface in solution of 0.1 M Py and 0.1 M $LiClO_4$. The surface of the electrode is covered with Py layer. The low sharpness of the image shows that this outer layer is very soft. In order to examine the structure of the Py layer in more detail we dissolved outer, probably softer part of the Py layer and continued experiments only with inner part of the adsorbed Py layer.

Fig. 4, and Fig. 5 show AFM images of the Au (111) electrodes surfaces covered with Py after exposing them in solution containing 0.1 M of Py and 0.1 M of $LiClO_4$ and after rinsing them with MilliQ+ water. Images in Fig. 4 are taken *in-situ* in 0.1 M $LiClO_4$ solution, but images in Fig. 5 are taken *ex-situ* in air atmosphere after drying the samples. These images show clearly that the surfaces of the electrodes are fully covered with an adsorbed Py layer, but the character of the layer in liquid and in air is somewhat different. Essential increase of the root-mean-square (RMS) roughness values calculated for *in-situ* and *ex-situ* measured electrode surfaces comparing to RMS value calculated for bare Au (111) electrode surface, also confirms the presence of an adsorbed layer of Py (see Tab.1). Homogeneous surface coverage with Py nanoislands with diameter of~20 nm and height of 1–2 nm was investigated in dried conditions.

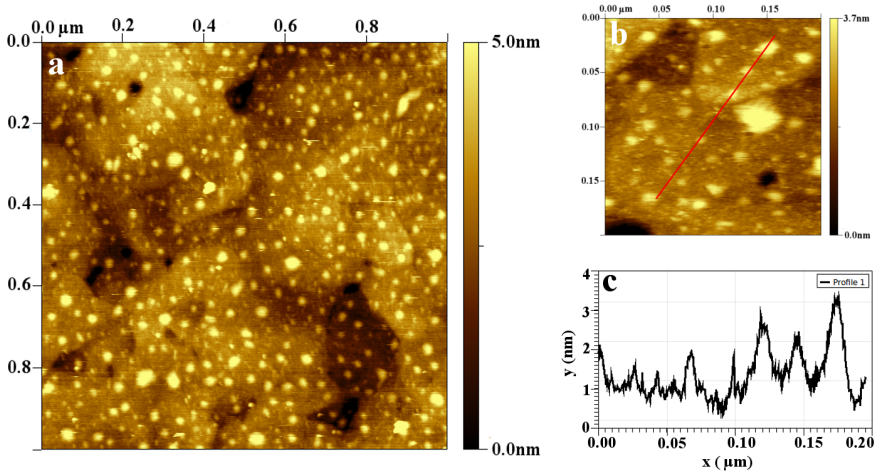

Fig. 4. *In-situ* non-contact AFM images (a,b) and cross-section profile (c) of adsorbed Py layer on Au(111) electrode measured in solution of 0.1 M $LiClO_4$ after rinsing in water.

Table 1. RMS roughness data for Py adsorbed layer and polymerised Py adsorbed layer.

	RMS (nm)				
Scanned area (µm)	Bare Au (111)	Adsorbed Py layer *in-situ*	Adsorbed Py layer dried	Polymerised Py layer *in-situ*	Polymerised Py layer dried
1x1	0.17	0.73	0.70	1.09	0.69

In liquid environment, the adsorbed layer consists of bigger or smaller nano-islands too with diameter from 10 to 50 nm, but there can be found also tiny chain or fibre like protrusions. The latter ones could be linear monomer clusters or accidentally generated oligomer chains, e.g. caused by adsorbed light quanta or by any other stray source. It is a remarkable tendency, that both the nano-islands and other small details of the adsorbed layer are imaged in liquid with less sharper borders than in dried condition in air. This shows, that the adhesion of the adsorbed material onto the Au (111) electrode is rather weak, as even very small interactive forces generated by oscillating tip of the AFM cantilever sensor working in the non-contact mode are capable to somewhat disturb the layer.

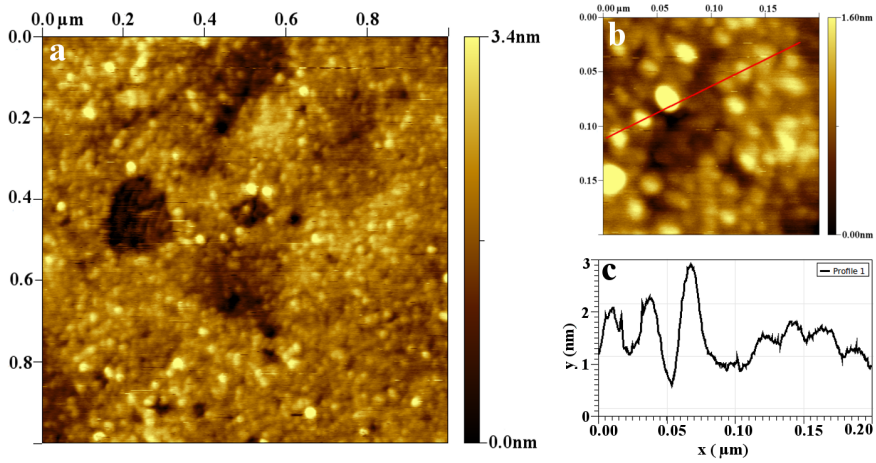

Fig. 5. *Ex-situ* non-contact AFM images (a,b) and cross-section profile (c) of adsorbed onto Au (111) electrode Py layer.

Electropolymerisation of adsorbed layer of Py was carried out in 0.1 M $LiClO_4$ solution with potential sweep from 0.0V to 0.75 V with scan rate 50 $mV \cdot s^{-1}$ and it causes remarkable changes in the morphology of this layer (Fig.-s 6 and 7). Nanoislands of diameter > 10 nm mostly disappear and a pre-structure of well-known cauliflower-like morphology of PPy appear [20,43,46,79,80]. This pre-structure consists of sub-micrometer aggregates of polymer nanoglobules, having diameter of 5–10 nm (see Fig. 7b), and this aggregates are concentrated preferable near the edges of substrate terraces – especially well visible in Fig. 7 part a, in which also the substrate structure is well imaged. Similar aggregates are present in the polymer layer imaged in the electrolyte environment (Fig. 6 part a) but there the edges are surrounded with a thinner fibre-like layer, which in some places has honeycomb-like structure, see Fig. 6 part b. Differently orientated fibril layers were observed in initial stages of PPy growth on HOPG also by Yang, Evans et al. [13]. Why the fibre-like structure is absent in the Fig. 7 part *a* is not clear yet – it is possible that during the layer drying process the thinner part of it was modified or even exfoliated from the electrode.

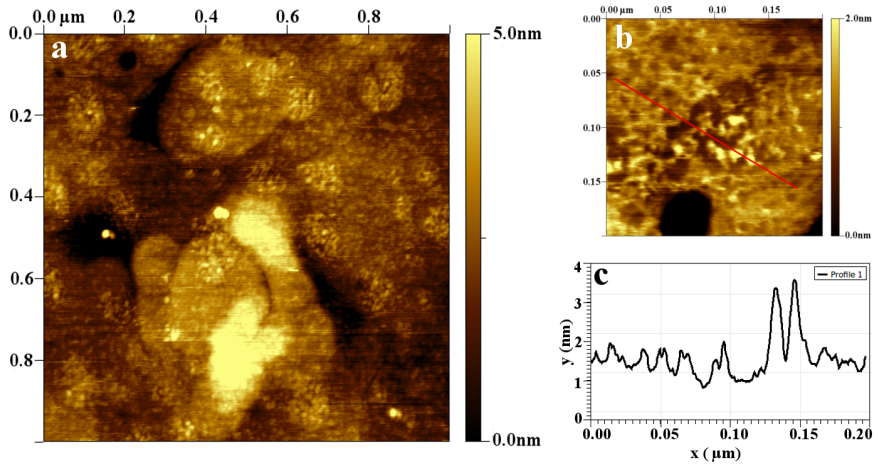

Fig. 6. *In-situ* non-contact AFM images (a,b) and cross-section profile (c) of electro-polymerised Py-adlayer on Au (111) electrode.

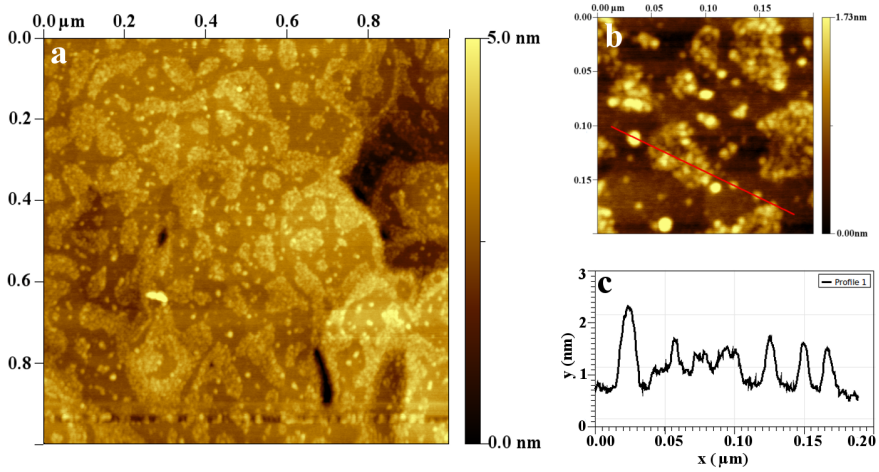

Fig. 7. *Ex-situ* non-contact AFM images (a,b) and cross-section profile (c) of electro-polymerised Py-adlayer on Au (111) electrode.

4.2. Formation of PPy film on Au (111): A STM and XPS Study

4.3. Dependence of PPy film morphology on different dopant anions.

The morphology of PPy films doped with different anions was studied by NC-AFM and IC-AFM. The PPy films were electrochemically deposited on gold wire electrode. Thickness of these films was ~ 1 μm. All experiments were carried out *ex-situ* in ambient conditions.

Differences in PPy film morphology, synthesised in the same conditions, were investigated using very different by size dopant ions – Cl^- and $TPPS_4$. The electropolymerisation of PPy films were carried out from two different aqueous solutions: 0.1 M Py + 0.1 M NaCl; and 0.1 M Py + 2 mM $TPPS_4$ + 0.1 M NaCl. PPy films were deposited on gold wire electrode during potential sweep from +0.45 V to +0.7 V with v= 1 $mV \cdot s^{-1}$. AFM images of these PPy films are presented in Fig.15. From these images it is clear that $TPPS_4$ substantially changes the morphology of the surface making it rougher, thus increasing the effective surface of the polymer layer. PPy/Cl film shows uniform globular structure with globule size from 30 nm to 80 nm, and RMS roughness 4.5 nm, but PPy/$TPPS_4$ films surface consists of disordered fibre like structures. RMS roughness of PPy/$TPPS_4$ film was 27.5 nm.

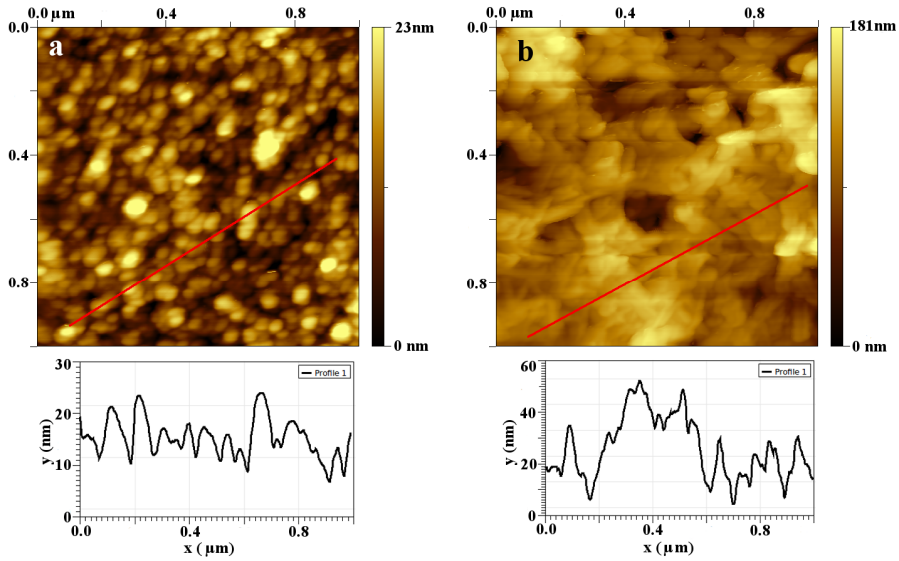

Fig. 15. *Ex-situ* IC-AFM images and cross-section profiles of PPy films on gold wire electrodes formed during potential sweep from +0.45 V to +0.7 V with v= 1 $mV \cdot s^{-1}$ in aqueous solution of: (a) 0.1 M Py + 0.1 M NaCl; (b) 0.1 M Py + 2 mM $TPPS_4$ + 0.1 M NaCl.

Investigations of differences in morphology of PPy films doped with relatively similar aromatic sulphonate anions have been done using IC-AFM. All PPy films for the AFM measurements were prepared in the same conditions: by galvanostatic electropolymerisation in aqueous solutions containing 0.1 M of Py and 0.1 M of supporting electrolyte: NaBS, Na*p*-TS or NaNDS. Typical surface images are presented in Fig. 16 and the values of the RMS roughness parameter and the dimensions of larger globules are presented in Table 2. From Fig. 16 and Table 2 one can see that the roughness parameter depends on the dimensions of the area used. If large globules are excluded (scanned area 1 µm x 1 µm), the RMS is relatively low. If large globules are included (scanned area 6 µm x 6 µm) values of RMS are much larger. But in all cases the PPy films doped with NDS^- have larger roughness. At the same time, the globules are largest on the surface of the PPy/NDS films. All this is supporting the statement that PPy films doped with NDS^- anions have a more heterogeneous structure.

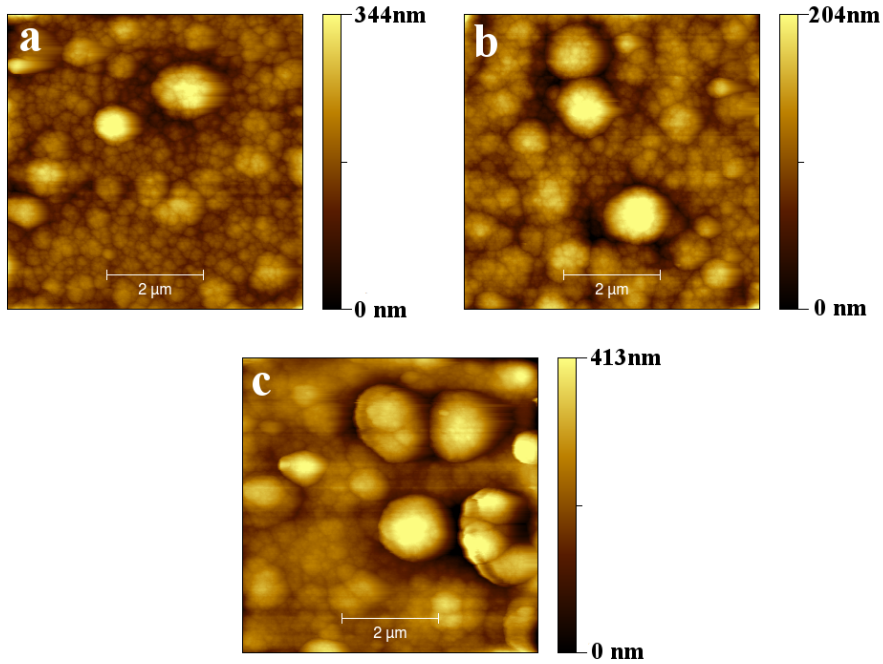

Fig. 16. *Ex-situ* AFM images from the surface of PPy films doped with BS (a), pTS (b) and NDS (c).

Table 2. AFM data for PPy films with various dopant anions.

	BS^-	*p*-TS^-	NDS^-
Scanned area (µm)	RMS (nm)		
6×6	45	45	106
1×1	13	15	30
Globule height (nm)	245	203	278
Globule width (nm)	1300	1200	1400

Possible changes in the morphology of the BS^- doped PPy films on the thickness and electrodeposition rate were also studied. PPy films for AFM measurements were prepared by galvanostatic electropolymerisation in aqueous solutions containing 0.1 M of Py and 0.1 M of supporting electrolyte: NaBS. In these experiments, PPy films were deposited at two current densities: 0.4 and at 4 $mA \cdot cm^{-2}$ with the total charge passed 0.08 $C \cdot cm^{-2}$ and 0.4 $C \cdot cm^{-2}$. Considering that about 0.4 $C \cdot cm^{-2}$ is consumed for the deposition of 1 µm thick films [74,92], the estimated thickness of the PPy films is approximately 0.2 and 1.0 µm. The typical AFM images are presented in Figs. 17 and 18. In the case of the thinner films (deposition charge 80 $mC \cdot cm^{-2}$), the morphology depends

rather weakly upon the deposition current density: the values of the roughness factor RMS are close: 4.4 and 4.6 nm in the case deposition current of 4.0 and 0.4 mA·cm^{-2}, respectively.

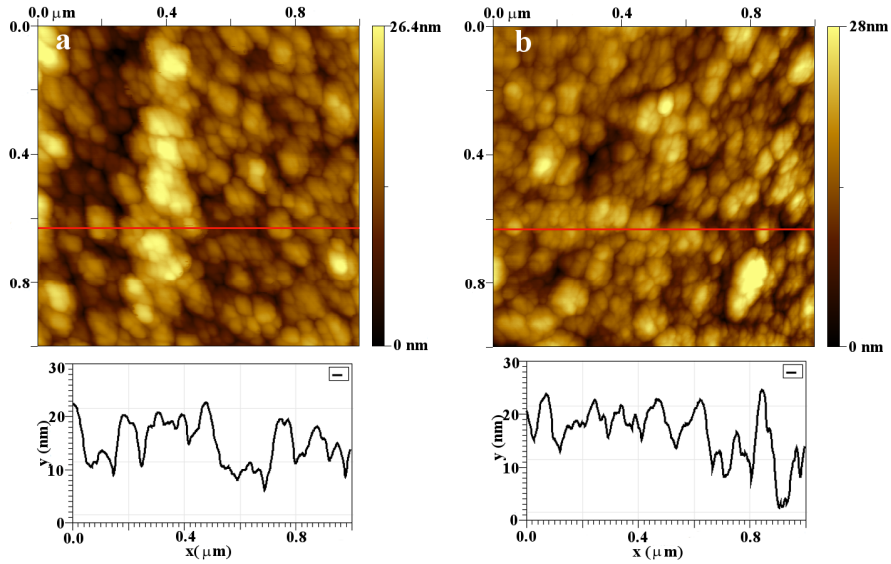

Fig. 17. AFM images of PPy/BS film deposited at current density: (a) jd = 0.4 mA·cm^{-2}; Qd = 400 mC·cm^{-2} and (b) j_d = 4.0 mA·cm^{-2}; Q_d = 400 mC·cm^{-2}.

The differences increase with the increase of the thickness of the film: the larger globules of "cauliflowers" reach 0.8 µm for the PPy films deposited at 0.4 mA·cm^{-2} versus only 0.5 µm if the deposition current was 4.0 mA·cm^{-2}. AFM measurements of PPy/BS thicker films morphology, synthesised in the different conditions using two different current densities, show that higher synthesis current density changes the morphology of the surface making it rougher.

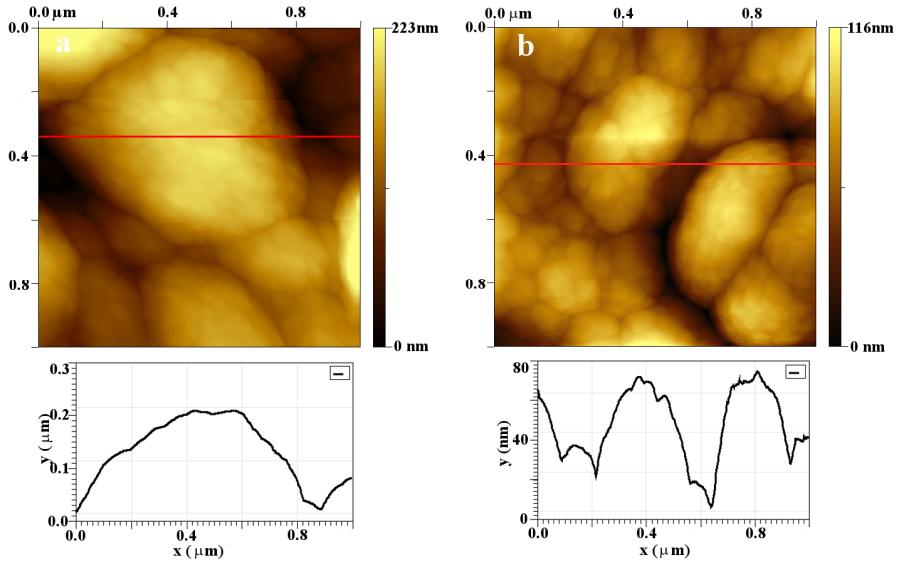

Fig. 18. AFM images of PPy/BS film deposited at current density: (a) j_d = 0.4 mA·cm^{-2}; Q_d = 80mC·cm^{-2} and (b) j_d = 4.0mA·cm^{-2}; Q_d = 80mC·cm^{-2}.

5. SUMMARY

The aim of the present work was to investigate the first stage of polypyrrole (PPy) growth for better understanding of the film formation mechanisms, and also the study of the dependences of PPy film morphology on the nature of dopant anions. For these purposes, electrochemically polymerised PPy films were used. Morphology of these films was studied by scanning probe microscopy (SPM). The essential results of these investigations can be listed as follows:

- In- and *ex-situ* atomic force microscopy (AFM) measurements in non-contact imaging mode showed that Au (111) electrode surface is covered with a polymolecular layer of pyrrole (Py). This layer is not ideally smooth but is formed from Py nanoislands with diameter of 10–50 nm and height of 1–3 nm.
- Electropolymerisation of this layer causes some typical changes: the nanoislands of diameter > 10 nm mostly disappear, and fibre-like or honeycomb-like structure appears. This new structure is formed not from single polymer chains but is more coarse-fibred.
- The results of *in-situ* AFM measurements showed clearly that the formation of the primary PPy layers during electropolymerisation from Py solutions of moderate concentration occurs from Py molecules previously adsorbed on the electrode.
- *In-situ* scanning tunneling microscopy (STM) studies of ultrathin PPy films deposited from aqueous Na_2SO_4 solution and low concentrations of Py onto Au (111) showed that in the first step of electrodeposition, the electrode still tends to be covered with continuous ultrathin adsorbate film as it was shown by *in-situ* AFM experiments.
- It was shown that the ultrathin polymer films can be studied in detail with *in-situ* STM if the polymer chains are bonded to the substrate surface with the help of sulphate ions adsorbed together with the first adsorbate species, improving their adhesion.
- Using the STM technique, then island-like growth of PPy film on the continuous adsorbate sublayer was demonstrated for the first time.
- Comparison of *ex-situ* and *in-situ* STM images of the same galvanostatically deposited films showed that in dry conditions the island material has lower electrical conductivity than the continuous layer.
- X-ray photoelectron spectroscopy (XPS) studies showed that PPy films synthesized galvanostatically from concentrated Py solutions contains a remarkable amount of sulphate anions as dopants, while films synthesized with the same amount of charge but from diluted Py solution had no dopant but contained carboxyl groups instead, thus were overoxidized.
- AFM measurements of PPy film morphology, synthesised in the same conditions using very differently sized dopant ions – Cl^- and $TPPS_4$, show

clearly that $TPPS_4$ substantially changes the morphology of the surface making it rougher.

- AFM investigations of differences in the morphology of PPy films doped with relatively similar aromatic sulphonate anions (BS^-, *p*-TS^- and NDS^-) synthesised in the same conditions show that PPy films doped with NDS^- anions have a more heterogeneous structure.
- The AFM experiments showed increased globularity for thicker films deposited at higher current densities in case of BS^- doped PPy films synthesised under different conditions.

Galvanostatic deposition of PPy from diluted solutions of Py under conditions of the parallel overoxidation reaction taking place allows the single-step production of nanometric overoxidised PPy films applicable in various sensors.

6. REFERENCES

1. T. A. Skotheim. Handbook of conducting Polymers. Vol 1. MARCEL DEKKER, INC. 1986.
2. G. G. Wallace. G.M. Spinks. Conductive electroactive polymers. Intelligent Materials Systems. 2003. CRC Press LLC.227.
3. T. F. Otero; M. Sansiňena. Adv.Mater. 10 (1998) 491.
4. F. Vidal, C. Plesse, D. Teyssié, C. Chevrot. Synthetic Metals 142 (2004) 287.
5. J. Li, X.-Q. Lin, Anal. Chim. Acta 596 (2007) 222.
6. C. Debiemme-Chouvy, Electrochem. Solid-State Lett. 10 (2007) E24.
7. C. Debiemme-Chouvy, Biosens. Bioelectron. 25 (2010) 2454.
8. S. Sadki, P. Schottland, N. Brodie, G. Sabouraud, Chem. Soc. Rev. 29 (2000) 283.
9. J. Heinze, B. A. Frontana-Uribe, S. Ludwigs, Chem. Rew. 110 (2010) 4724.
10. E. L. Florin, M. Radmacher, B. Fleck, and H. E. Gaub, Rev. Sci. Instrum. 65 (1993) 639.
11. W. Han, S. M. Lindsay, T. Jing, Appl. Phys. Lett. 69 (1996) 4111.
12. W. Han, Ultramicroscopy 108 (2008) 1009.
13. R. Yang, D. F. Evans, L. Christensen, W. A. Hendrickson, J. Phys. Chem. 94 (1990) 6117.
14. G. Caple, B. L. Wheeler, R. Swift, T. L. Porter, S. Jeffers, J. Phys. Chem. 94 (1990) 5641.
15. B. J. Hwang, R. Santhanam, Y. L. Lin, Electroanalysis 15 (2003) 115.
16. B. J. Hwang, R. Santhanam, Y. L. Lin, Electrochim. Acta 46 (2001) 2843.
17. A. Kaynak, Mater. Res. Bull. 32 (1997) 271.
18. Y. S. Cohen, M.D. Levi, D. Aurbach, Langmuir 19 (2003) 9804.
19. K. Idla, A. Talo, H. E.-M. Niemi, O. Forsén, S. Yläsaari, Surf. Interf. Anal. 25 (1997) 837.
20. A. C. Cascalheira, A. S. Viana, L. M. Abrantes, Electrochim. Acta 53 (2008) 5783.
21. J. N. Barisci, R. Stella, G. M. Spinks, G. G. Wallace, Electrochim. Acta 46 (2000) 519.
22. A. Malinauskas, Polymer 42 (2001) 3957.
23. G. B. Street, T. C. Clarke, M. Krounbi, K. K. Kanazawa, V. Lee, P. Pfluger, J. C. Scott, G. Weiser, Mol. Cryst. Liq. Cryst. 83 (1982) 253.
24. E. M. Genies, G. Bidan, A. F. Diaz, J. Electroanal. Chem. 149 (1983) 101.
25. B. L. Flunt, A. F. Diaz, Organic Electrochemictry: an Introduction and Guide, Marcel Dekker, New York, 1991.
26. M. Salmon, A. F. Diaz, A. J. Logan, M. Krounbi, J. Bargon, Mol. Cryst. Liq. Cryst. 83 (1982) 1297.
27. A. Mohammadi, O. Inganas, I. Lundström, J. Electrochem. Soc. 133 (1986) 947.
28. D. A. Kaplin, S. Qutubuddin, Polymer 36 (1995) 1275.
29. J. M. Ko, H. W. Dee, S.-M. Park, C. Y. Kim, J. Electrochem. Soc. 137 (1990) 905.
30. J. S. Shapiro, W. T. Smith, Polymer 34 (1993) 4336.
31. B. R. Saunders, K. S. Murray, R. J. Fleming, Y. Korbatieh, Chem. Mater. 5 (1993) 809.
32. L. Fang, T. Y. Dai, Y. Lu, Synth. Met. 159 (2009) 2101.
33. M. F. Suárez, R. G. Compton, J. Electroanal. Chem. 462 (1999) 211.

34. J. Li, E. Wang, Synth. Met. 66 (1994) 67.
35. J. Li, E. Wang, M. Green, P. E. West, Synth. Met. 74 (1995) 127.
36. E. Lacaze, J. Garbarz, V. Quillet, M. Schott, M.C. Pham, J. Moslih, P.C. Lacaze, Ultramicroscopy 42–44 (1992) 1037.
37. R. Yang, K. M. Dalsin, D. F. Evans, L. Christensen, W. A. Hendrickson, J. Phys. Chem. 93 (1989) 511.
38. R. Yang, K. Naoi, D. F. Evans, W. H. Smyrl, W. A. Hendrickson, Langmuir 7 (1991) 556.
39. M. P. Everson, J. H. Helms, Synth. Met. 40 (1991) 97.
40. T. L. Porter, C. Y. Lee, B. L. Wheeler, G. Caple, J. Vac. Sci. Tehnol. A 9 (1991) 1452.
41. M.F. Suarez-Herrera, J.M. Feliu, Phys. Chem. Chem. Phys. 10 (2008) 70220.
42. H. J. Lee, S.-M. Park, J. Phys. Chem. B 109 (2005) 13247.
43. D.-H. Han, H. J. Lee, S.-M. Park, Electrochim. Acta 50 (2005) 3085.
44. H. J. Lee, S.-M. Park, J. Phys. Chem. B 108 (2004) 1590.
45. T. Silk, Q. Hong, J. Tamm, R. G. Compton, Synth. Met. 93 (1998) 59.
46. T. Silk, Q. Hong, J. Tamm, R. G. Compton, Synth. Met. 93 (1998) 65.
47. R. Wiesendanger. Scanning Probe Microscopy: Analytical Methods. Berlin: Springer Verlag, 1998.
48. M.E. Greene, C.R. Kinser, D.E. Kramer, L. S. C. Pingree, M. C. Hersam, Microscopy Research Technique 64 (2004) 415.
49. Y. F. Dufrene, Nature Reviews, Microbiology 2 (2004) 451.
50. R. A. Oliver, Rep. Prog. Phys. 71 (2008) 076501.
51. G. Ge, D. Han, D. Lin, W. Chua, Y. Sun, L. Jiang, W. Ma, C. Wang, Ultramicroscopy 107 (2007) 299.
52. I. Revenko, R. Proksch, J. Appl. Phys. 87 (2000) 526.
53. W. Han, S. M. Lindsay, Appl. Phys. Lett. 72 (1998) 1656.
54. A.-M. Chiorcea, A.M. Oliveira-Brett, Bioelectrochemistry 55 (2002) 63.
55. J. Wiedemair, M. J. Serpe, J. Kim, J.-F. Masson, L. A. Lyon, B. Mizaikoff, C. Kranz, Langmuir 23 (2007) 130.
56. K. Itaya, Prog. Surf. Sci. 58 (1998) 121.
57. H. Siegenthaler, in Scanning Tunnelling Microscopy II, R. Wiesendanger, H.-J. Guntherodt (Eds.), Springer Verlag, Berlin 1992 p.7.
58. J. Clavilier, R. Faure, G. Guinet, R. Durand, J. Electroanal. Chem. 107 (1979) 205.
59. A. Hamelin, in Modern Aspects of Electrochemistry, No. 16, B. E. Conway, R. E. White, J, O'M. Bockris (Eds.), Plenum Press, New York, 1985, p.1.
60. S. Motoo, N. Furuya, J. Electroanal. Chem. 167 (1984) 309.
61. K. Sashikata, N. Furuya, K. Itaya, J. Vac. Sci. Technol. B9 (1991) 457.
62. P. Sobotik, I. Ost'adal, J. Cryst. Growth 197 (1999) 955.
63. I. Ost'adal, P. Sobotik, Czech. J. Phys. 47 (1997) 445.
64. X.-Y. Zheng, Y. Ding, L.A. Bottomley, D.P. Allison, R.J. Warmack, J. Vac. Sci. Technol. B 13 (1995) 1320.
65. Z.H. Liu, N.M. D. Brown, Thin Solid Films 300 (1997) 84.
66. N. J. Tao, J. A. DeRose, S. M. Lindsay, J. Phys. Chem. 97 (1993) 910.
67. G. Yang, L. Tan, Y. Yang, S. Chen, G.-Y. Liu, Surf. Sci. 589 (2005) 129.
68. A. Sarapuu, S. Kallip, A. Kasikov, L. Matisen, K. Tammeveski, J. Electroanal. Chem. 624 (2008) 144.

69. S. Wakamatsu, J. Nakada, S. Fujii, U. Akiba,M. Fujihira, Ultramicroscopy 105 (2005) 26.
70. M. H. Dishner, J. C. Hemminger, F. J. Feher, Langmuir 12 (1996) 6176.
71. F. Cunha, N. J. Tao, X. W. Wang, Q. Jin, J. DAgnese, Langmuir 12 (1996) 6410.
72. S. J. Park, R.E. Palmer, Phys. Rev. Lett. 102 (2009) 216805.
73. V. Krishna, Y. H. Ho, S. Basak, K. Rajeshwar, J. Am. Chem. Soc. 113 (1991) 3325.
74. A.F. Diaz, J.I. Castillo, J.A. Logan, W.Y. Lee, J. Electroanal. Chem. 129 (1981) 115.
75. http://gwyddion.net/
76. I. Horcas, R. Fernandez, J.M. Gomez-Rodriguez, J. Colchero, J. Gomez-Herrero, A. M. Baro, Rev. Sci. Instrum. 78 (2007) 013705.
77. C. D. Wagner, L. E. Davis, M. V. Zeller, J. A. Tailor, R. H. Raymond, L. H. Gale, Surf. Interf. Anal. 3 (1981) 211.
78. http://www.cem.msu.edu/~cem924sg/XPSASFs.html
79. J. Tamm, T. Raudsepp, M. Marandi, T. Tamm, Synth. Met. 157 (2007) 66.
80. T. Raudsepp, M. Marandi, T. Tamm, V. Sammelselg, J. Tamm. Electrochim. Acta 53 (2008) 3828.
81. A. Cuesta, M. Kleinert, D. M. Kolb, Phys. Chem. Chem. Phys. 2 (2000) 5684.
82. M. Marandi, J. Tamm, V. Sammelselg, E-MRS 2007 Fall Meeting, Book of Abstracts 2007, 264.
83. B. J. Hwang, R. Santhanam, Y. L. Lin, Electrochim. Acta 46 (2001) 2843.
84. R. Erlandsson, O. Inganas, I. Lundström, W. R. Salaneck, Synth. Met. 10 (1985) 303.
85. http://www.lasurface.com/database/elementxps.php
86. P. Pfluger, M. Krounbi, G. B. Street, G. Weiser, J. Chem. Phys. 78 (1983) 3212.
87. R. Erlandsson, I. Lundström, J. Phys. (Paris), Colloq. 44 (1983) C3 – 713.
88. F. Beck, U. Barsch, R. Michaelis, J. Electroanal. Chem. 351 (1993) 169.
89. R. Ansari, E-Journal of Chemistry 3 (2006) 186.
90. A. Madani, B. Nessark, R. Brayner, H. Elaissari, M. Jouini, C. Mangeney, M. Chehimi, Polymer 51 (2010) 2825.
91. R. Rajagopalan, J.O. Iroh, Appl. Surf. Sci. 218 (2003) 58.
92. A.F. Diaz, J.M. Vasquez Vallejo, A. Martinez Duran, IBM J. Res. Dev. 25 (1981) 42.

SUMMARY IN ESTONIAN

POLÜPÜRROOLKILEDE ELEKTROFORMEERUMINE: *IN-SITU* AFM JA STM UURINGUD

Elektrit juhtivaid polümeere on viimaste aastakümnete jooksul intensiivselt uuritud kui uut orgaaniliste materjalide generatsiooni, milles on metallidele ja pooljuhtidele omased elektrilised ja optilised omadused ühendatud tava-polümeeride selliste omadustega nagu lihtne süntees ja paindlikkus töötlemisel. Polüpürrooli (PPy) peetakse üheks elektrit juhtivate polümeeride klassikaliseks esindajaks tänu selle püsivusele ja võimalusele seda polümeeri kergelt sünteesida nii keemiliselt kui elektrokeemiliselt vesi- ning orgaanilistest lahustest. PPy-d kasutatakse juba paljudes kõrgtehnoloogilistes rakendustes, näiteks, keemiliste- ja biosensorite, päiksepatareide, akude, korrosioonitõrje katete, superkondensaatorite, molekulaarsõelte, jne valmistamisel. Samuti loetakse polüpürrooli lootustandvaks materjaliks kunstlihaste valmistamisel.

Käesoleva töö eesmärgiks oli uurida polüpürrooli kile moodustumist, sealhulgas ka pürrooli (Py) adsorbtsiooni monokristalsetel Au (111) elektroodidel erineva pürrooli sisaldusega vesilahustest ning erinevate dopantioonide mõju kile pinna struktuurile paksemates polüpürrooli kiledes. Uuringud viidi läbi erinevaid *in-* ja *ex-situ* skaneeriva teravikmikroskoopia ning röntgen-fotoelektron-spektroskoopia (XPS) meetodeid kasutades.

Olulisemad tulemused:

- *In-* ja *ex-situ* aatomjõu mikroskoopia (AFM) mõõtmiste tulemusena näidati, et 0.1 M Py vesilahuses on Au (111) elektroodi pind kaetud polümolekulaarse Py kihiga. See kiht ei ole ideaalselt sile vaid koosneb Py saarekestest mõõtudega: 10–50 nm diameeter ja 1–3 nm kõrgus.
- *In-situ* AFM mõõtmised näitasid kindlalt, et mõõduka kontsentratsiooniga Py lahustes elektropolümeriseerimise käigus tekkivad esimesed PPy kihid moodustatakse eelnevalt elektroodile adsorbeerunud molekulidest.
- Näidati, et üliõhukesi PPy kilesid on võimalik *in-situ* skaneeriva tunnelmikroskoopia (STM) meetodil detailselt uurida kui elektroodi pinnale adsorbeerunud polümeeri ahelad on sulfaatioonide abil tugevamini substraadi pinnaga seotud.
- Esmakordselt näidati PPy kile saarelist kasvu pideval adsorbsel kihil kasutades STM-i.
- Galvanostaatiliselt sünteesitud PPy kilede XPS uuringutel tehti kindlaks, et kontsentreeritumast (0.1M) Py lahusest sadestatud kiled sisaldavad märkimisväärsel hulgal dopantiooni, samas kui väiksema Py kontsentratsiooniga (1mM) lahusest samadel tingimustel sadestatud kiledes dopantiooni ei leitud vaid need sisaldasid karbonüülrühmi, mis näitab, et viimatimainitud kiled olid üleoksüdeeritud.

- Suhteliselt „paksude“ kilede (kuni 1 μm) AFM uuringud näitasid, et sünteesitingimuste muutmine, dopantiooni iseloom ja kile paksus mõjutavad tugevalt kile pinna struktuuri.

Uuringute käigus avastati uus väga lihtne meetod üliõhukeste üleoksüdeeritud kilede valmistamiseks. Niisugused kiled on kasutatavad erinevates sensorites.

ACKNOWLEDGEMENTS

I wish to express my gratitude to my doctoral advisors Prof. Jüri Tamm and Prof. Väino Sammelselg for the professional guidance and advice they provided through the years of collaboration.

I am very thankful to all my friends and colleagues for helpful discussions, inspiration and continuous support.

Especially I would like to thank Dr. Urmas Johanson, who invited me to the world of conducting polymers, and Dr. Silvar Kallip, who introduced me to the Scanning Probe Microscopy.

I wish to thank Dr. Tarmo Tamm for good discussions and help in preparing manuscripts.

Dr. Terje Raudsepp is specially acknowledged for good advice and company.

Also, I am very thankful to my colleagues in Institute of Physics for their support and good advice on terms of gold evaporation, and XPS measurements.

Last but not least, I would thank my family for continuous support during the long years of my studies.

PUBLICATIONS

CURRICULUM VITAE

MARGUS MARANDI

General Data

Born: March 6, 1970, Viljandi
Citizenship: Estonian
Address: University of Tartu
Institute of Chemistry
Ravila 14 A, Tartu, 50411, Estonia.
Phone: (+ 371) 737 5171
E-mail: margus.marandi@ut.ee

Education

2004–... University of Tartu, PhD student (in chemistry)
2001–2004 University of Tartu, graduate student, MSc
1997–2001 University of Tartu, student, BSc
1977–1988 Viljandi 5th Secondary School

Work experience

2008–… University of Tartu, Faculty of Science and Technology, Institute of Physics, University of Tartu, Laboratory of of Thin-Film Technology; Researcher (0.80)
2008–2009 University of Tartu, Faculty of Science and Technology, Dean's Office, Doctoral school of material science and material technology; Extraordinary Researcher (0.08)
2007–2008 University of Tartu, Faculty of Science and Technology, Institute of Physics, University of Tartu; insener (0.30)

Publications

1. **Marandi, M.**; Kallip, S.; Sammelselg, V.; Tamm, J.; AFM study of the adsorption of pyrrole and formation of the polypyrrole film on gold surface. Electrochem. Commun. 12(6) (2010) 854–858.
2. Raudsepp, T.; **Marandi, M.**; Tamm, T.; Sammelselg, V.; Tamm, J.; Redoping – A simple way to enhance the redoxcapasity of polypyrrole films; Electrochem. Commun. 12 (2010) 1180–1183.

3. Kullapere, M.; Marandi, M.; Sammelselg, V.; Menezes, H.A.; Maia, G.; Tammeveski, K.; Surface modification of gold electrodes with anthraquinone diazonium cations. Electrochem. Commun 11(2) (2009) 405–408.
4. Kruusenberg, I.; **Marandi, M.**; Sammelselg, V.; Tammeveski, K.; Hydrodynamic deposition of carbon nanotubes onto HOPG: The reduction of oxygen on CNT/HOPG electrodes in alkaline solution. Electrochemical and Solid State Letters 12(11) (2009). F31–F34.
5. Raudsepp, T.; **Marandi. M.**; Tamm,T.; Sammelselg, V.; Tamm, J.; Study of the factors determining the mobility of ions in the polypyrrole films doped with aromatic sulfonate anions. Electrochim. Acta. 53 (2008) 3828–3835.
6. Tamm, J.; Raudsepp, T.; **Marandi, M.**; Tamm, T.; Electrochemical Properties of the Polypyrrole Films Doped with Benzenesulfonate, Synth. Met. 157(2007) 66–73.
7. Johanson, U.; **Marandi, M.**; Tamm, T.; Tamm, J.; Comparative study of the behavior of anions in polypyrrole films. Electrochimica Acta 50(7–8) (2005) 1523–1528.
8. Johanson, U.; **Marandi, M.**; Sammelselg, V.; Tamm, J.; Electrochemical properties of porphyrin-doped polypyrrole films. J. Electroanal. Chem. 575(2),(2005) 267–273.
9. Tamm, J.; Johanson, U.; **Marandi, M.**; Tamm, T.; Tamm, L.; Study of the properties of electrodeposited polypyrrole films. Russian Journal of Electrochemistry 40(3) (2004) 344–348.
10. Kullapere, M.; **Marandi, M.**; Matisen, L.; Mirkhalaf, F.; Carvalho, A. E.; Maia, G.; Sammelselg, V.; Tammeveski, K.; Blocking properties of gold electrodes modified with 4-nitrophenyl and 4-decylphenyl groups. J. Solid State Electrochem. (2011) accepted.
11. Raudsepp, T.; **Marandi, M.**; Tamm, T.; Sammelselg, V.; Tamm, J.; Influence of redoping on electrochemical properties of the polypyrrole films; Electrochim. Acta submitted.
12. **Marandi, M.**; Kallip, S.; Matisen, L.; Tamm, J.; Sammelselg, V.; Formation of Nanometric Polypyrrole Films on Au (111): a STM, SEM and XPS Study. Langmuir submitted.

ELULOOKIRJELDUS

MARGUS MARANDI

Üldandmed

Sünniaeg ja koht: 06. märts 1970, Viljandi
Kodakondsus: Eesti
Kontakt: Tartu Ülikool
Keemia Instituut
Ravila 14 A, Tartu, 50411, Eesti.
Telefon: (+ 371) 737 5171
E-mail: margus.marandi@ut.ee

Haridus

2004–...	Tartu Ülikool doktorant
2001–2004	Tartu Ülikool magistrant, keemiamagister, MSc 2004
1997–2001	Tartu Ülikool üliõpilane, keemiabakalaureus, BSc 2001
1977–1988	Viljandi V Keskkool

Teenistuskäik

2008	Tartu Ülikool, Loodus- ja tehnoloogiateaduskond, Tartu Ülikooli Füüsika Instituut, Kiletehnoloogia labor; Teadur 0.80)
2008–2009	Tartu Ülikooli Loodus-ja tehnoloogiateaduskond, Loodus- ja tehnoloogiateaduskonna dekanaat, Materjaliteaduse ja materjalide tehnoloogia doktorikool; Erakorraline teadur (0.08)
2007–2008	Tartu Ülikool, Loodus- ja tehnoloogiateaduskond, Tartu Ülikooli Füüsika Instituut; insener (0.30)

Teadustööde loetelu

Teaduslikud artiklid rahvusvahelise levikuga väljaannetes:

1. **Marandi, M.**; Kallip, S.; Sammelselg, V.; Tamm, J.; AFM study of the adsorption of pyrrole and formation of the polypyrrole film on gold surface. Electrochem. Commun. 12(6) (2010) 854–858.
2. Raudsepp, T.; **Marandi, M.**; Tamm, T.; Sammelselg, V.; Tamm, J.; Re-doping – A simple way to enhance the redoxcapasity of polypyrrole films; Electrochem. Commun. 12 (2010) 1180–1183.

3. Kullapere, M.; Marandi, M.; Sammelselg, V.; Menezes, H.A.; Maia, G.; Tammeveski, K.; Surface modification of gold electrodes with anthraquinone diazonium cations. Electrochem. Commun. 11(2) (2009) 405–408.
4. Kruusenberg, I.; **Marandi, M.**; Sammelselg, V.; Tammeveski, K.; Hydrodynamic deposition of carbon nanotubes onto HOPG: The reduction of oxygen on CNT/HOPG electrodes in alkaline solution. Electrochemical and Solid State Letters 12(11) (2009). F31–F34.
5. Raudsepp, T.; **Marandi. M.**; Tamm,T.; Sammelselg, V.; Tamm, J.; Study of the factors determining the mobility of ions in the polypyrrole films doped with aromatic sulfonate anions. Electrochim. Acta. 53 (2008) 3828 -3835.
6. Tamm, J.; Raudsepp, T.; **Marandi, M.**; Tamm, T.; Electrochemical Properties of the Polypyrrole Films Doped with Benzenesulfonate, Synth. Met. 157(2007) 66–73.
7. Johanson, U.; **Marandi, M.**; Tamm, T.; Tamm, J.; Comparative study of the behavior of anions in polypyrrole films. Electrochimica Acta 50(7–8) (2005) 1523–1528.
8. Johanson, U.; **Marandi, M.**; Sammelselg, V.; Tamm, J.; Electrochemical properties of porphyrin-doped polypyrrole films. J. Electroanal. Chem. 575(2),(2005) 267–273.
9. Tamm, J.; Johanson, U.; **Marandi, M.**; Tamm, T.; Tamm, L.; Study of the properties of electrodeposited polypyrrole films. Russian Journal of Electrochemistry 40(3) (2004) 344–348.
10. Kullapere, M.; **Marandi, M.**; Matisen, L.; Mirkhalaf, F.; Carvalho, A. E.; Maia, G.; Sammelselg, V.; Tammeveski, K.; Blocking properties of gold electrodes modified with 4-nitrophenyl and 4-decylphenyl groups. J. Solid State Electrochem. (2011) accepted.
11. Raudsepp, T.; **Marandi, M.**; Tamm, T.; Sammelselg, V.; Tamm, J.; Influence of redoping on electrochemical properties of the polypyrrole films; Electrochim. Acta submitted.
12. **Marandi, M.**; Kallip, S.; Matisen, L.; Tamm, J.; Sammelselg, V.; Formation of Nanometric Polypyrrole Films on Au (111): a STM, SEM and XPS Study. Langmuir submitted.

DISSERTATIONES CHIMICAE UNIVERSITATIS TARTUENSIS

1. **Toomas Tamm.** Quantum-chemical simulation of solvent effects. Tartu, 1993, 110 p.
2. **Peeter Burk.** Theoretical study of gas-phase acid-base equilibria. Tartu, 1994, 96 p.
3. **Victor Lobanov.** Quantitative structure-property relationships in large descriptor spaces. Tartu, 1995, 135 p.
4. **Vahur Mäemets.** The ^{17}O and ^{1}H nuclear magnetic resonance study of H_2O in individual solvents and its charged clusters in aqueous solutions of electrolytes. Tartu, 1997, 140 p.
5. **Andrus Metsala.** Microcanonical rate constant in nonequilibrium distribution of vibrational energy and in restricted intramolecular vibrational energy redistribution on the basis of slater's theory of unimolecular reactions. Tartu, 1997, 150 p.
6. **Uko Maran.** Quantum-mechanical study of potential energy surfaces in different environments. Tartu, 1997, 137 p.
7. **Alar Jänes.** Adsorption of organic compounds on antimony, bismuth and cadmium electrodes. Tartu, 1998, 219 p.
8. **Kaido Tammeveski.** Oxygen electroreduction on thin platinum films and the electrochemical detection of superoxide anion. Tartu, 1998, 139 p.
9. **Ivo Leito.** Studies of Brønsted acid-base equilibria in water and non-aqueous media. Tartu, 1998, 101 p.
10. **Jaan Leis.** Conformational dynamics and equilibria in amides. Tartu, 1998, 131 p.
11. **Toonika Rinken.** The modelling of amperometric biosensors based on oxidoreductases. Tartu, 2000, 108 p.
12. **Dmitri Panov.** Partially solvated Grignard reagents. Tartu, 2000, 64 p.
13. **Kaja Orupõld.** Treatment and analysis of phenolic wastewater with microorganisms. Tartu, 2000, 123 p.
14. **Jüri Ivask.** Ion Chromatographic determination of major anions and cations in polar ice core. Tartu, 2000, 85 p.
15. **Lauri Vares.** Stereoselective Synthesis of Tetrahydrofuran and Tetrahydropyran Derivatives by Use of Asymmetric Horner-Wadsworth-Emmons and Ring Closure Reactions. Tartu, 2000, 184 p.
16. **Martin Lepiku.** Kinetic aspects of dopamine D_2 receptor interactions with specific ligands. Tartu, 2000, 81 p.
17. **Katrin Sak.** Some aspects of ligand specificity of P2Y receptors. Tartu, 2000, 106 p.
18. **Vello Pällin.** The role of solvation in the formation of iotsitch complexes. Tartu, 2001, 95 p.

19. **Katrin Kollist.** Interactions between polycyclic aromatic compounds and humic substances. Tartu, 2001, 93 p.
20. **Ivar Koppel.** Quantum chemical study of acidity of strong and superstrong Brønsted acids. Tartu, 2001, 104 p.
21. **Viljar Pihl.** The study of the substituent and solvent effects on the acidity of OH and CH acids. Tartu, 2001, 132 p.
22. **Natalia Palm.** Specification of the minimum, sufficient and significant set of descriptors for general description of solvent effects. Tartu, 2001, 134 p.
23. **Sulev Sild.** QSPR/QSAR approaches for complex molecular systems. Tartu, 2001, 134 p.
24. **Ruslan Petrukhin.** Industrial applications of the quantitative structure-property relationships. Tartu, 2001, 162 p.
25. **Boris V. Rogovoy.** Synthesis of (benzotriazolyl)carboximidamides and their application in relations with *N*- and *S*-nucleophyles. Tartu, 2002, 84 p.
26. **Koit Herodes.** Solvent effects on UV-vis absorption spectra of some solvatochromic substances in binary solvent mixtures: the preferential solvation model. Tartu, 2002, 102 p.
27. **Anti Perkson.** Synthesis and characterisation of nanostructured carbon. Tartu, 2002, 152 p.
28. **Ivari Kaljurand.** Self-consistent acidity scales of neutral and cationic Brønsted acids in acetonitrile and tetrahydrofuran. Tartu, 2003, 108 p.
29. **Karmen Lust.** Adsorption of anions on bismuth single crystal electrodes. Tartu, 2003, 128 p.
30. **Mare Piirsalu.** Substituent, temperature and solvent effects on the alkaline hydrolysis of substituted phenyl and alkyl esters of benzoic acid. Tartu, 2003, 156 p.
31. **Meeri Sassian.** Reactions of partially solvated Grignard reagents. Tartu, 2003, 78 p.
32. **Tarmo Tamm.** Quantum chemical modelling of polypyrrole. Tartu, 2003. 100 p.
33. **Erik Teinemaa.** The environmental fate of the particulate matter and organic pollutants from an oil shale power plant. Tartu, 2003. 102 p.
34. **Jaana Tammiku-Taul.** Quantum chemical study of the properties of Grignard reagents. Tartu, 2003. 120 p.
35. **Andre Lomaka.** Biomedical applications of predictive computational chemistry. Tartu, 2003. 132 p.
36. **Kostyantyn Kirichenko.** Benzotriazole — Mediated Carbon–Carbon Bond Formation. Tartu, 2003. 132 p.
37. **Gunnar Nurk.** Adsorption kinetics of some organic compounds on bismuth single crystal electrodes. Tartu, 2003, 170 p.
38. **Mati Arulepp.** Electrochemical characteristics of porous carbon materials and electrical double layer capacitors. Tartu, 2003, 196 p.

39. **Dan Cornel Fara.** QSPR modeling of complexation and distribution of organic compounds. Tartu, 2004, 126 p.
40. **Riina Mahlapuu.** Signalling of galanin and amyloid precursor protein through adenylate cyclase. Tartu, 2004, 124 p.
41. **Mihkel Kerikmäe.** Some luminescent materials for dosimetric applications and physical research. Tartu, 2004, 143 p.
42. **Jaanus Kruusma.** Determination of some important trace metal ions in human blood. Tartu, 2004, 115 p.
43. **Urmas Johanson.** Investigations of the electrochemical properties of polypyrrole modified electrodes. Tartu, 2004, 91 p.
44. **Kaido Sillar.** Computational study of the acid sites in zeolite ZSM-5. Tartu, 2004, 80 p.
45. **Aldo Oras.** Kinetic aspects of dATPαS interaction with $P2Y_1$ receptor. Tartu, 2004, 75 p.
46. **Erik Mölder.** Measurement of the oxygen mass transfer through the air-water interface. Tartu, 2005, 73 p.
47. **Thomas Thomberg.** The kinetics of electroreduction of peroxodisulfate anion on cadmium (0001) single crystal electrode. Tartu, 2005, 95 p.
48. **Olavi Loog.** Aspects of condensations of carbonyl compounds and their imine analogues. Tartu, 2005, 83 p.
49. **Siim Salmar.** Effect of ultrasound on ester hydrolysis in aqueous ethanol. Tartu, 2006, 73 p.
50. **Ain Uustare.** Modulation of signal transduction of heptahelical receptors by other receptors and G proteins. Tartu, 2006, 121 p.
51. **Sergei Yurchenko.** Determination of some carcinogenic contaminants in food. Tartu, 2006, 143 p.
52. **Kaido Tämm.** QSPR modeling of some properties of organic compounds. Tartu, 2006, 67 p.
53. **Olga Tšubrik.** New methods in the synthesis of multisubstituted hydrazines. Tartu. 2006, 183 p.
54. **Lilli Sooväli.** Spectrophotometric measurements and their uncertainty in chemical analysis and dissociation constant measurements. Tartu, 2006, 125 p.
55. **Eve Koort.** Uncertainty estimation of potentiometrically measured ph and pK_a values. Tartu, 2006, 139 p.
56. **Sergei Kopanchuk.** Regulation of ligand binding to melanocortin receptor subtypes. Tartu, 2006, 119 p.
57. **Silvar Kallip.** Surface structure of some bismuth and antimony single crystal electrodes. Tartu, 2006, 107 p.
58. **Kristjan Saal.** Surface silanization and its application in biomolecule coupling. Tartu, 2006, 77 p.
59. **Tanel Tätte.** High viscosity $Sn(OBu)_4$ oligomeric concentrates and their applications in technology. Tartu, 2006, 91 p.

60. **Dimitar Atanasov Dobchev**. Robust QSAR methods for the prediction of properties from molecular structure. Tartu, 2006, 118 p.
61. **Hannes Hagu**. Impact of ultrasound on hydrophobic interactions in solutions. Tartu, 2007, 81 p.
62. **Rutha Jäger.** Electroreduction of peroxodisulfate anion on bismuth electrodes. Tartu, 2007, 142 p.
63. **Kaido Viht.** Immobilizable bisubstrate-analogue inhibitors of basophilic protein kinases: development and application in biosensors. Tartu, 2007, 88 p.
64. **Eva-Ingrid Rõõm.** Acid-base equilibria in nonpolar media. Tartu, 2007, 156 p.
65. **Sven Tamp.** DFT study of the cesium cation containing complexes relevant to the cesium cation binding by the humic acids. Tartu, 2007, 102 p.
66. **Jaak Nerut.** Electroreduction of hexacyanoferrate(III) anion on Cadmium (0001) single crystal electrode. Tartu, 2007, 180 p.
67. **Lauri Jalukse.** Measurement uncertainty estimation in amperometric dissolved oxygen concentration measurement. Tartu, 2007, 112 p.
68. **Aime Lust.** Charge state of dopants and ordered clusters formation in CaF_2:Mn and CaF_2:Eu luminophors. Tartu, 2007, 100 p.
69. **Iiris Kahn**. Quantitative Structure-Activity Relationships of environmentally relevant properties. Tartu, 2007, 98 p.
70. **Mari Reinik.** Nitrates, nitrites, N-nitrosamines and polycyclic aromatic hydrocarbons in food: analytical methods, occurrence and dietary intake. Tartu, 2007, 172 p.
71. **Heili Kasuk.** Thermodynamic parameters and adsorption kinetics of organic compounds forming the compact adsorption layer at Bi single crystal electrodes. Tartu, 2007, 212 p.
72. **Erki Enkvist.** Synthesis of adenosine-peptide conjugates for biological applications. Tartu, 2007, 114 p.
73. **Svetoslav Hristov Slavov**. Biomedical applications of the QSAR approach. Tartu, 2007, 146 p.
74. **Eneli Härk.** Electroreduction of complex cations on electrochemically polished Bi(*hkl*) single crystal electrodes. Tartu, 2008, 158 p.
75. **Priit Möller.** Electrochemical characteristics of some cathodes for medium temperature solid oxide fuel cells, synthesized by solid state reaction technique. Tartu, 2008, 90 p.
76. **Signe Viggor.** Impact of biochemical parameters of genetically different pseudomonads at the degradation of phenolic compounds. Tartu, 2008, 122 p.
77. **Ave Sarapuu.** Electrochemical reduction of oxygen on quinone-modified carbon electrodes and on thin films of platinum and gold. Tartu, 2008, 134 p.
78. **Agnes Kütt.** Studies of acid-base equilibria in non-aqueous media. Tartu, 2008, 198 p.

79. **Rouvim Kadis.** Evaluation of measurement uncertainty in analytical chemistry: related concepts and some points of misinterpretation. Tartu, 2008, 118 p.
80. **Valter Reedo.** Elaboration of IVB group metal oxide structures and their possible applications. Tartu, 2008, 98 p.
81. **Aleksei Kuznetsov.** Allosteric effects in reactions catalyzed by the cAMP-dependent protein kinase catalytic subunit. Tartu, 2009, 133 p.
82. **Aleksei Bredihhin.** Use of mono- and polyanions in the synthesis of multisubstituted hydrazine derivatives. Tartu, 2009, 105 p.
83. **Anu Ploom.** Quantitative structure-reactivity analysis in organosilicon chemistry. Tartu, 2009, 99 p.
84. **Argo Vonk.** Determination of adenosine A_{2A}- and dopamine D_1 receptor-specific modulation of adenylate cyclase activity in rat striatum. Tartu, 2009, 129 p.
85. **Indrek Kivi.** Synthesis and electrochemical characterization of porous cathode materials for intermediate temperature solid oxide fuel cells. Tartu, 2009, 177 p.
86. **Jaanus Eskusson.** Synthesis and characterisation of diamond-like carbon thin films prepared by pulsed laser deposition method. Tartu, 2009, 117 p.
87. **Margo Lätt.** Carbide derived microporous carbon and electrical double layer capacitors. Tartu, 2009, 107 p.
88. **Vladimir Stepanov.** Slow conformational changes in dopamine transporter interaction with its ligands. Tartu, 2009, 103 p.
89. **Aleksander Trummal.** Computational Study of Structural and Solvent Effects on Acidities of Some Brønsted Acids. Tartu, 2009, 103 p.
90. **Eerold Vellemäe.** Applications of mischmetal in organic synthesis. Tartu, 2009, 93 p.
91. **Sven Parkel.** Ligand binding to 5-HT_{1A} receptors and its regulation by Mg^{2+} and Mn^{2+}. Tartu, 2010, 99 p.
92. **Signe Vahur.** Expanding the possibilities of ATR-FT-IR spectroscopy in determination of inorganic pigments. Tartu, 2010, 184 p.
93. **Tavo Romann**. Preparation and surface modification of bismuth thin film, porous, and microelectrodes. Tartu, 2010, 155 p.
94. **Nadežda Aleksejeva.** Electrocatalytic reduction of oxygen on carbon nanotube-based nanocomposite materials. Tartu, 2010, 147 p.
95. **Marko Kullapere.** Electrochemical properties of glassy carbon, nickel and gold electrodes modified with aryl groups. Tartu, 2010, 233 p.
96. **Liis Siinor.** Adsorption kinetics of ions at Bi single crystal planes from aqueous electrolyte solutions and room-temperature ionic liquids. Tartu, 2010, 101 p.
97. **Angela Vaasa.** Development of fluorescence-based kinetic and binding assays for characterization of protein kinases and their inhibitors. Tartu 2010, 101 p.

98. **Indrek Tulp.** Multivariate analysis of chemical and biological properties. Tartu 2010, 105 p.
99. **Aare Selberg.** Evaluation of environmental quality in Northern Estonia by the analysis of leachate. Tartu 2010, 117 p.
100. **Darja Lavõgina.** Development of protein kinase inhibitors based on adenosine analogue-oligoarginine conjugates. Tartu 2010, 248 p.
101. **Laura Herm.** Biochemistry of dopamine D_2 receptors and its association with motivated behaviour. Tartu 2010, 156 p.
102. **Terje Raudsepp.** Influence of dopant anions on the electrochemical properties of polypyrrole films. Tartu 2010, 112 p.